

# Producing Positive, Negative, and No Cooperativity by Mutations at a Single Residue Located at the Subunit Interface in the Aspartate Receptor of *Salmonella typhimurium*<sup>†</sup>

Andrew F. Kolodziej, Thomas Tan, and Daniel E. Koshland, Jr.\*

Department of Molecular and Cell Biology, 229 Stanley Hall, University of California, Berkeley, Berkeley, California 94720

Received June 20, 1996; Revised Manuscript Received August 27, 1996<sup>⊗</sup>

**ABSTRACT:** Site-directed mutagenesis of the aspartate receptor of *Salmonella typhimurium* (Tar<sub>S</sub>)<sup>1</sup> at serine 68, a residue located within the aspartate binding pocket and at the subunit interface, identified this residue as an allosteric switch in this receptor. Substitutions at this position can affect both the type and degree of binding cooperativity observed. Negative cooperativity is observed in the wild-type receptor ( $n_H = 0.7 \pm 0.1$ ) and is maintained by the mutations S68C ( $n_H = 0.8 \pm 0.02$ ), S68V ( $n_H = 0.9 \pm 0.05$ ), and S68D (half-of-the-sites). Binding at only half of the sites was detectable in the S68D mutant, an extreme form of negative cooperativity. No cooperativity ( $n_H = 1.0 \pm 0.03$ ) was observed in the mutant S68A. Positive cooperativity was generated by the substitutions S68T ( $n_H = 1.2 \pm 0.09$ ), S68L ( $n_H = 1.2 \pm 0.1$ ), S68N ( $n_H = 1.3 \pm 0.2$ ), and S68I ( $n_H = 1.4 \pm 0.2$ ). Binding measurements indicated that the substitutions S68Q, S68E, and S68F decrease affinity of the first ligand binding 500-fold, 7000-fold, and 1600-fold, respectively.

Cooperativity is a widely observed and important regulatory component in biological systems. Cooperativity in proteins is generally mediated by changes at a subunit interface, and models have been developed that account for general types of binding behavior (Monod et al., 1965; Koshland et al., 1966). Recent efforts have focused on providing a structural basis for cooperative binding mechanisms and on detailing the interactions responsible for conferring allosteric properties to a protein. Delineating the structural changes accompanying ligand binding has been possible for some important positively cooperative proteins where the protein crystal structure has been determined in the presence and absence of substrate or effector binding. These studies have mainly focused on comparisons of unligated beginning and ligand-bound end states. Some examples are deoxy- and oxyhemoglobin (Perutz, 1970), apo- and *N*-(phosphoacetyl)-*L*-aspartate-bound aspartate transcarbamoylase (Krause et al., 1987; Ke et al., 1988; Kantrowitz & Lipscomb, 1990), and apo- and substrate-bound forms of fructose-1,6-bisphosphatase (Zhang et al., 1994) and glycogen phosphorylase (Barford & Johnson, 1989; Browner et al., 1994). Intermediate states of ligand binding, however, cannot be isolated in positively cooperative proteins because many states of binding site occupancy and subunit structure are present simultaneously. Insight into the structure of these states in hemoglobin has been obtained by NMR of cross-linked, modified hemoglobins, and these studies have supported the existence of intermediate ligation states (Miura & Ho, 1982, 1984; Miura et al., 1987; Ho, 1992). X-ray crystallographic data on intermediate states, however, have been acquired only indirectly where a beginning or end state

has been perturbed by binding of an allosteric activator or inhibitor, as in aspartate transcarbamoylase (Stevens et al., 1990; Gouaux et al., 1990; Stevens & Lipscomb, 1992; Kossman et al., 1993).

The opportunity to correlate the structure of an intermediate state with cooperative binding occurs more favorably in a negatively cooperative protein, because, depending on the extent of negative cooperativity, discrete states can be observed and studied. One such example is the aspartate receptor of *Salmonella typhimurium*, a dimeric receptor that binds aspartate with negative cooperativity. The structure of the ligand binding domain has been solved in three states: an apo state, an intermediate state with one aspartate bound per dimer (the half-of-the-sites form) (Milburn et al., 1991; Yeh et al., 1993), and a state where both sites are occupied (Yeh et al., 1996). The contribution of individual residues to cooperativity and ligand affinity can also be analyzed by mutagenesis, an approach that has been useful for dissecting allosteric mechanisms in hemoglobin and aspartate transcarbamoylase (Valdes & Ackers, 1977; Perutz et al., 1987; Stevens et al., 1991; Ishimori et al., 1992).

The X-ray structures have provided a detailed picture of the protein contacts involved in aspartate binding and intersubunit interactions (Figure 1) (Milburn et al., 1991; Yeh et al., 1993, 1996). Some of the residues involved in binding are located at the subunit interface since the binding pockets are composed of residues from both subunits. The side chains of Arg69' and Arg73' from the opposite subunit (residues contributed by the opposite subunit are designated with a prime symbol) extend into the binding pocket and form strong electrostatic bonds with the  $\alpha$ -carboxyl and  $\gamma$ -carboxyl groups of the ligand aspartate. Substitutions at these positions reduce ligand affinity 100–1000-fold (Kossman et al., 1988; Wolff & Parkinson, 1988; Mowbray et al., 1990; Gardina et al., 1992). A third residue that has been implicated in aspartate binding and that is located at the subunit interface is Ser68. This residue is positioned

<sup>†</sup> Research supported by NIH Grant DK09765 to D.E.K., a postdoctoral fellowship from the Damon Runyon–Walter Winchell Cancer Fund to A.F.K., and the W. M. Keck Foundation to D.E.K.

\* Corresponding author.

<sup>⊗</sup> Abstract published in *Advance ACS Abstracts*, November 1, 1996.

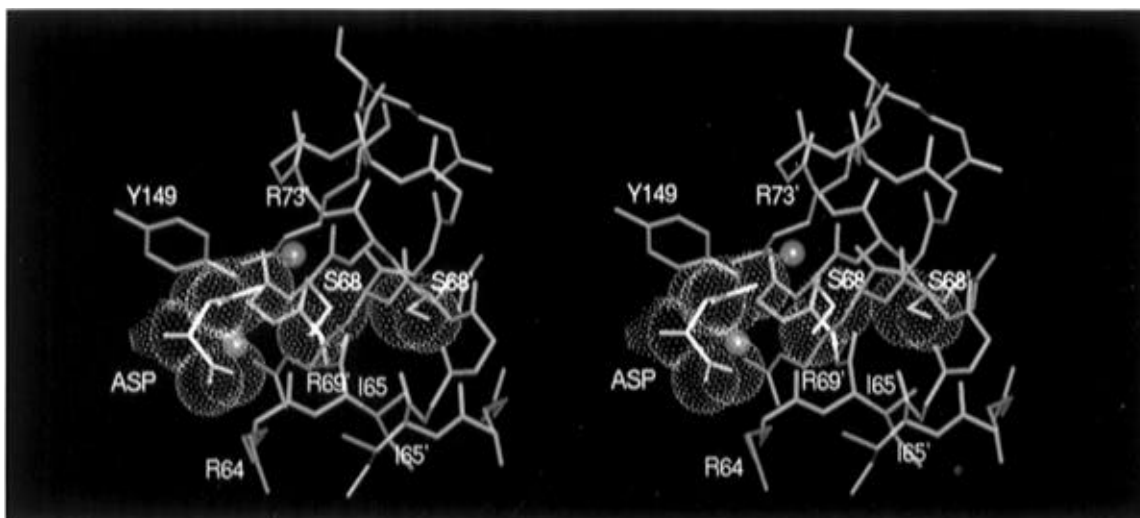


FIGURE 1: Stereo image of the X-ray crystal structure of the occupied aspartate binding site in the half-of-the-sites form. The structure shown is the binding site of the wild-type periplasmic domain where one of the two binding sites is occupied by aspartate (orange), as reported by Yeh et al. (1993). The second site (not shown) is occupied by water molecules. The backbone atoms of the two helices forming the subunit interface (pink) and the side chains of residues involved in aspartate binding (magenta) are displayed. Water molecules are displayed as green spheres. Van der Waals surfaces are displayed for aspartate and the side chains of Ser68 and Ser68'.

opposite Ser68' (in the half-of-the-sites form,  $d_{O\beta-O\beta'} = 4.73$  Å and  $d_{C\beta-C\beta'} = 3.34$  Å). Although the side chain hydroxyl group of Ser68 is 5.3 Å from the  $\gamma$ -carboxylate oxygen of the bound aspartate, it binds aspartate indirectly via interactions with two bound water molecules (Milburn et al., 1991). The  $\beta$ -hydroxyl of Ser68 points inward toward the binding site where it makes a weak hydrogen bond with one water molecule ( $d_{O\beta-O} = 3.9$  Å) that is hydrogen bonded both to the  $\gamma$ -carboxylate of the bound aspartate ( $d_{O-O} = 3.0$  Å) and to the hydroxyl of Tyr149 ( $d_{O-O} = 3.2$  Å). The second water molecule forms a hydrogen-bonding bridge between Ser68 ( $d_{O\beta-O} = 3.1$  Å) and the  $\alpha$ -carboxylate of aspartate ( $d_{O-O} = 2.6$  Å) and also hydrogen bonds to Tyr149 ( $d_{O-O} = 2.7$  Å). The contribution to aspartate binding by Ser68 has not been directly evaluated, although a role is suggested by identification of a S68I point mutation in Tar<sub>E</sub><sup>1</sup> that reduces aspartate chemotaxis by 40% and decreases aspartate affinity by about 10-fold (Gardina et al., 1992).

Due to its unique location both within the ligand binding site and at the dimer interface, it seemed likely that Ser68 could also have a significant role in mediating negative cooperativity within the receptor through its interactions with both the substrate and the opposite subunit. We have tested the function of Ser68 by introducing a number of substitutions at this site and analyzing their effects on ligand binding and cooperativity. We demonstrate here that Ser68 is integral to the allosteric switching mechanism in this receptor, and mutations at this position shed light on the general mechanism of allosteric effects.

## EXPERIMENTAL PROCEDURES

**Strains and Plasmids.** *Escherichia coli* strain RP4080 (*cheR217*) and *E. coli* RP8611 [ $\Delta$ (tsr)(DE7028)  $\Delta$ (tar-tap)-DE5201 zbd::Tn5  $\Delta$ (trg)-DE100] were kindly provided by

Dr. Sandy Parkinson, University of Utah (Liu & Parkinson, 1989). *E. coli* strain HCB721 [ $\Delta$ (tsr)7021 trg::Tn10  $\Delta$ (cheA-cheY)::XhoI (Tn5)] was generously provided by Dr. Howard Berg, Harvard University (Wolfe et al., 1988). *E. coli* strain CJ236 (*dut ung*) was purchased from Bio-Rad. Wild-type and mutant receptors were expressed from the plasmid pEMBLtar<sub>s</sub> (Falke & Koshland, 1987). The parent plasmid pEMBL18 (Dente et al., 1983) was from Boehringer Mannheim.

**Site-Directed Mutagenesis.** Site-directed mutagenesis of pEMBLtar<sub>s</sub> was performed according to the method of Kunkel (1985). Single-stranded, uracil-enriched template was made in *E. coli* strain CJ236 from pEMBLtar<sub>s</sub> using helper phage M13K07 (Bio-Rad Corp.). Using reagents and methods provided in the MutaGene kit (Bio-Rad Corp.), oligonucleotides (20–30 bp in length) bearing the appropriate mutation were annealed to the template, and strand synthesis was accomplished with T7 polymerase and T4 ligase. Following transformation into *E. coli* strain XL-2 (Stratagene), colonies were screened for plasmids bearing the mutation by restriction mapping or DNA sequencing. DNA sequencing was performed by the dideoxy nucleotide chain termination method using Taq polymerase (Innis et al., 1988) and reagents supplied in the dsDNA Cycle Sequencing System (GibcoBRL). The presence of all mutations was confirmed by DNA sequencing at the mutated site and flanking regions ( $\pm 50$  bp).

**Membrane Preparation.** Membranes of RP4080 and HCB721 expressing the *S. typhimurium* aspartate receptor were prepared as previously described (Foster et al., 1985). Membranes were suspended in final buffer (10% glycerol, 5 mM EDTA, 1 mM PMSF, 50 mM Tris, pH 7.5) at a volume of 1 mL/g cell paste, aliquoted in 1 mL volumes, and stored at  $-80$  °C for up to 6 months.

**Quantitation of Receptors.** To measure receptor concentrations in membranes, samples from the aspartate binding assays were diluted appropriately and compared on SDS-PAGE gels (Laemmli, 1970) to five dilutions of an aspartate receptor standard (in the range of 0.1–0.5 mg/mL; 100–500 ng of total protein per lane). The gels were stained with

<sup>1</sup> Abbreviations: CheR, S-adenosylmethionine-dependent methyl transferase;  $n_H$ , Hill coefficient; SDS-PAGE, sodium dodecyl sulfate-polyacrylamide gel electrophoresis; Tar<sub>E</sub>, *Escherichia coli* aspartate receptor; Tar<sub>S</sub>, *Salmonella typhimurium* aspartate receptor.

Coomassie Brilliant Blue R250, dried between sheets of cellophane, and individual lanes were scanned with a laser densitometer (LKB). Relative band densities were determined from peak integration after background subtraction. Plots of band density vs protein mass were linear ( $R > 0.98$ ), and the concentration of the analyzed samples fell within the range of the standards. The standards were derived from a sample of wild-type aspartate receptor, purified to homogeneity as previously described (Biemann & Koshland, 1994). Amino acid analysis (UC Davis Microsequencing Facility, Davis, CA) was used to determine the concentration in an aliquot of the purified standard that was precipitated with 15% trichloroacetic acid, washed with acetone, and dried.

**Swarm Assays.** Swarm plate assays were used to characterize the ability of wild-type and mutant aspartate receptor to mediate chemotaxis in *E. coli* strain RP8611. Swarm assays were conducted on soft agar plates containing either 1% Bacto tryptone or 0.1 mM aspartate, as previously described (Weis & Koshland, 1990).

**Methylation Assays.** *In vitro* methylation reactions were conducted in buffer containing 10% glycerol, 50 mM sodium phosphate, pH 7.0, 1 mM EDTA, 2 mM 2-mercaptoethanol, 1 mM phenylmethanesulfonyl fluoride, and 1  $\mu$ M [ $^3$ H]-S-adenosylmethionine in the presence or absence of aspartate, as indicated in the Results section. Methyl transferase was prepared as a cell extract supernatant of *E. coli* strain RP3808 expressing the *cheR* gene product encoded by the plasmid pME43 (Simms et al., 1987), and a final dilution of 1:300 was used in each assay. Reactions were initiated by addition of a 2 $\times$  CheR cocktail to a sample of *E. coli* RP4080 membranes expressing wild-type or mutant receptor (10  $\mu$ M). The procedure for conducting the methylation reactions was as previously described (Shapiro & Koshland, 1994), and  $^3$ H incorporation was linear ( $R > 0.98$ ) between 0–5 min.

**Binding Assays of Membrane-Bound Receptors.** Binding assays were conducted at 4 °C essentially as previously described (Clarke et al., 1979; Biemann & Koshland, 1994). All mutants were expressed in *E. coli* strain RP4080, except S68D which was expressed in HCB721. Membranes containing aspartate receptor (100  $\mu$ L) were added to 100  $\mu$ L of final buffer containing various concentrations of L-[2,3- $^3$ H]aspartic acid (0.1 mCi/mmol; purchased from Amersham) from 0.3 to 100  $\mu$ M. After mixing, 95  $\mu$ L of the membrane mixture was added to tubes containing either 1  $\mu$ L of H<sub>2</sub>O (to determine the free aspartate concentration) or 1  $\mu$ L of 100 mM L-aspartate (to determine the total aspartate concentration). The samples were centrifuged at 150000g for 8 min in a TLA100 rotor (Beckman Instruments), and aspartate present in the supernatant was measured by scintillation counting of three 20  $\mu$ L aliquots. The bound aspartate concentration was determined by subtraction of free aspartate from total aspartate. Control experiments with RP4080 membranes derived from cells harboring the parent plasmid pEMBL18 or with RP4080 membranes containing receptors with low aspartate affinity ( $K_1' < 0.001 \mu\text{M}^{-1}$ ) indicated that the level of nonspecific binding was negligible.

**Data Analysis.** Aspartate binding data were analyzed in three ways: (a) Scatchard plots (Scatchard, 1949), (b) the Hill equation (Hill, 1910), and (c) the sequential ligand binding model (Koshland et al., 1966; Koshland, 1975). Scatchard analysis was accomplished by plotting the ratio

$N_B/S_F$  versus  $N_B$ , according to the equation:

$$\frac{N_B}{S_F} = K_H(2P_T - N_B) \quad (1)$$

$N_B$  is equal to  $S_B/P_T$ , where  $S_B$  represents the concentration of macromolecule sites occupied by ligand and  $P_T$  is the concentration of receptor. The aspartate receptor is composed of two initially identical binding sites, so the concentration of potentially available binding sites is  $2P_T$ , and  $N_B$  would converge at high substrate concentration to a value  $N_{B \max} = 2.0$  for full-sites ligand occupancy.  $S_F$  is the free ligand (aspartate) concentration, and  $K_H$  is the associative binding constant defined in the Hill equation (eq 2). Saturation plots of  $N_B$  versus  $S_F$  were fit to the Hill equation:

$$N_B = \frac{N_{B \max}(S_F)^{n_H}}{\frac{1}{K_H} + S_F^{n_H}} \quad (2)$$

where  $n_H$  is the Hill coefficient. Associative binding constants for the aspartate receptor (AR),  $K_1$  and  $K_2$ , were obtained by fitting the experimental binding data ( $N_B$  versus  $S_F$ ) to the sequential ligand binding model described by the equation:

$$N_B = \frac{K_1 S_F + 2K_1 K_2 S_F^2}{1 + K_1 S_F + K_1 K_2 S_F^2} \quad (3)$$

where

$$K_1 = \frac{[\text{AR} \cdot \text{Asp}_1]}{[\text{AR}][\text{Asp}]} \quad \text{and} \quad K_2 = \frac{[\text{AR} \cdot \text{Asp}_2]}{[\text{AR} \cdot \text{Asp}_1][\text{Asp}]} \quad (4)$$

For purposes of curve fitting, the coefficients in eq 3 were replaced by the variables  $\varphi_1$  and  $\varphi_2$  where

$$\varphi_1 = K_1 \quad \text{and} \quad \varphi_2 = K_1 K_2 \quad (5)$$

Because of statistical factors inherent to binding a ligand to a multimeric protein, the thermodynamic constants,  $K_1$  and  $K_2$ , must be modified to reflect the intrinsic binding affinity of each site (Koshland et al., 1966). The constants,  $K_1'$  and  $K_2'$ , are corrected for these statistical factors and express the inherent affinity of the individual sites for ligand:

$$K_1 = 2K_1' \quad \text{and} \quad K_2 = (1/2)K_2' \quad (6)$$

The statistical factors used to relate the measured constants ( $K_1$  and  $K_2$ ) to intrinsic constants ( $K_1'$  and  $K_2'$ ) are independent of mechanism and have no bias in mechanistic terms.

The protein concentration,  $P_T$ , occurs in the denominator of  $N_B$  and is estimated by gel densitometry measurements. To allow for errors in determining  $P_T$ , as well as ligand concentration, we fit the data to eq 7, using the parameters  $\varphi_1$  and  $\varphi_2$  (eq 5) and  $p_n$ .

$$N_B = \frac{p_n(K_1 S_F + 2K_1 K_2 S_F^2)}{1 + K_1 S_F + K_1 K_2 S_F^2} \quad (7)$$

All curve fitting was performed using the program Table Curve 2-D (AISN Software). Values obtained from averaging the fits to data from three or more individual binding

experiments (except S68D for which two trials were performed) and their standard deviations are reported.

To obtain values of  $K_{1/2}$  for aspartate binding to S68E, S68Q, and S68F, the rate of receptor methylation by CheR at a given aspartate concentration divided by the rate in the absence of aspartate ( $R$ ) was plotted as a function of aspartate concentration. Values of  $K_{1/2}$ , the concentration of aspartate required to reach half-maximum stimulation of receptor methylation, were calculated by fitting the points to the equation:

$$R = R_0 + \frac{(R_{\max} - R_0)(\text{Asp})}{K_{1/2} + (\text{Asp})} \quad (8)$$

where  $R_0$  and  $R_{\max}$  represent the enhancement of receptor methylation by aspartate at low (well below  $K_{1/2}$ ) and high (well above  $K_{1/2}$ ) aspartate concentrations.

**Molecular Modeling.** Molecular modeling of mutations was performed using the BioSym Software program INSIGHT for display functions, for construction of mutant receptors, and for producing Figures 1 and 6. The mutation residues were rotated to the most favorable rotamer conformations that minimized unfavorable van der Waals interactions and maintained favorable van der Waals interactions or by energy minimization using DISCOVER.

## RESULTS

**Cooperativity of Ligand Binding and Ligand Occupancy.** Given the unique positioning of Ser68 within the binding site and at the subunit interface, we believed that this residue could be important for mediating the negative cooperativity observed in aspartate binding. To assess its importance to the binding and signaling properties of the receptor, we have introduced 11 mutations at position 68, changing the native serine residue to aliphatic, acidic, and hydrogen-bonding residues: i.e., Ala, Val, Leu, Ile, Phe, Asp, Glu, Asn, Gln, Thr, and Cys. We measured aspartate binding to the membrane-associated form of each receptor and characterized their ability to mediate chemotaxis.

The mutant receptors were all expressed in *E. coli* at levels comparable to that of wild type (about 1 mg/g wet cell mass), and all were found to be associated with the membrane. Equilibrium aspartate binding reactions were performed on each mutant at high and low concentrations of receptor (4–40  $\mu\text{M}$ ), and the results were analyzed by three criteria: Scatchard analysis, binding fits to the Hill equation, and binding fits to the sequential binding model. The Scatchard plot was a useful qualitative tool to evaluate the type of cooperativity manifested by each mutant. The data were then correlated with eqs 2 and 7. Together, these different approaches should provide a coherent description of the binding cooperativity (Levitzki & Koshland, 1969), as summarized in Table 1.

In a system exhibiting cooperative behavior, the first ligand can induce conformational changes that increase (positive cooperativity) or decrease (negative cooperativity) the affinity of the second ligand bound to the subsequent site. The qualitative shape of the Scatchard plot for such a system provides an excellent indicator of the type of cooperativity in ligand binding and is related to the magnitude of the Hill coefficient,  $n_H$ , and the relative values of the intrinsic binding

Table 1: Diagnostic Results for Different Cooperativity Types in a Dimeric Protein

cooperativity type	Scatchard curve	Hill coeff	sequential model
positive	convex	$n_H > 1$	$K_1' < K_2'$
negative	concave	$n_H < 1$	$K_1' > K_2'$
no	linear	$n_H = 1$	$K_1' = K_2'$
half-of-the-sites	linear	$n_H = 1$	$K_1'(\text{observed}); K_2' = 0^a$

<sup>a</sup> Ligand occupancy is equal to 1.0.

constants  $K_1'$  and  $K_2'$  (Levitzki & Koshland, 1969; Dahlquist, 1978). Simulated Scatchard plots for systems showing either positive, negative, or no cooperativity are shown in Figure 2A. Positive cooperativity in ligand binding is characterized by a convex Scatchard plot showing a maximum, a Hill coefficient greater than one ( $n_H > 1.0$ ), and intrinsic binding constants  $K_1' < K_2'$ . On the other hand, negative cooperativity exhibits a concave, biphasic Scatchard plot, and the binding curve is described by a Hill coefficient less than one ( $n_H < 1.0$ ), and intrinsic binding constants  $K_1' > K_2'$ . Systems with multiple (independent) ligand affinities due to binding site heterogeneity may also exhibit a concave Scatchard plot which are distinguished from negative cooperativity by the purity of the protein and invariance of the binding constants in different preparations. Finally, a straight line Scatchard plot, a Hill coefficient equal to one ( $n_H = 1.0$ ), and intrinsic binding constants  $K_1' = K_2'$  are obtained when no cooperativity is present. A straight line Scatchard is also obtained for half-of-the-sites binding, an extreme form of negative cooperativity (Levitzki et al., 1971). The occupancy in this case is only half of the initially available sites. Klotz's criteria (Klotz, 1982) were used to assess if the available sites were saturated within the concentration range of the assay. For each mutant, a plateau in the Klotz plot ( $N_B$  vs  $\log[S_F]$ ) was observed at high substrate concentrations, indicating that saturating conditions were achieved.

Scatchard plots of all three types, convex, concave, and linear, were observed within the group of Ser68 mutants. Examples of each curve type derived from individual experiments are shown in Figure 2. For ease of interpretation, the theoretical curves for  $n_H = 0.7$ ,  $n_H = 1.0$ , and  $n_H = 1.5$  are shown in Figure 2A. The wild-type receptor exhibited a distinctly concave Scatchard plot (Figure 2B), indicative of negative cooperativity. Scatchard plots for the S68C mutant also displayed a concave curve similar to that of wild type (Figure 2C), and those for the S68V mutant had a less pronounced concavity, indicating weak negative cooperativity. The Scatchard plot for the S68I mutant (Figure 2D), on the other hand, had positive slope at low substrate concentration, peaked, and then gradually increased in negative slope, reflecting binding with positive cooperativity. The Scatchard plots of aspartate binding to S68N, S68T, and S68L were also convex. Scatchard plots for S68A were best fit to straight lines with  $N_{B \max}$  near 2.0 (Figure 2E), indicative of no cooperativity, whereas plots of S68D also gave straight lines, but with  $N_{B \max} = 1.0$ , a result consistent with half-of-the-sites binding in this mutant. No aspartate binding could be detected directly for the S68Q, S68E, and S68F mutants, indicating binding constants,  $K_1'$ , less than 0.02, the approximate sensitivity of our assay.

The qualitative results from the Scatchard plots are substantiated by quantitative fits of the data to the sequential ligand binding model (Koshland et al., 1966). The raw data

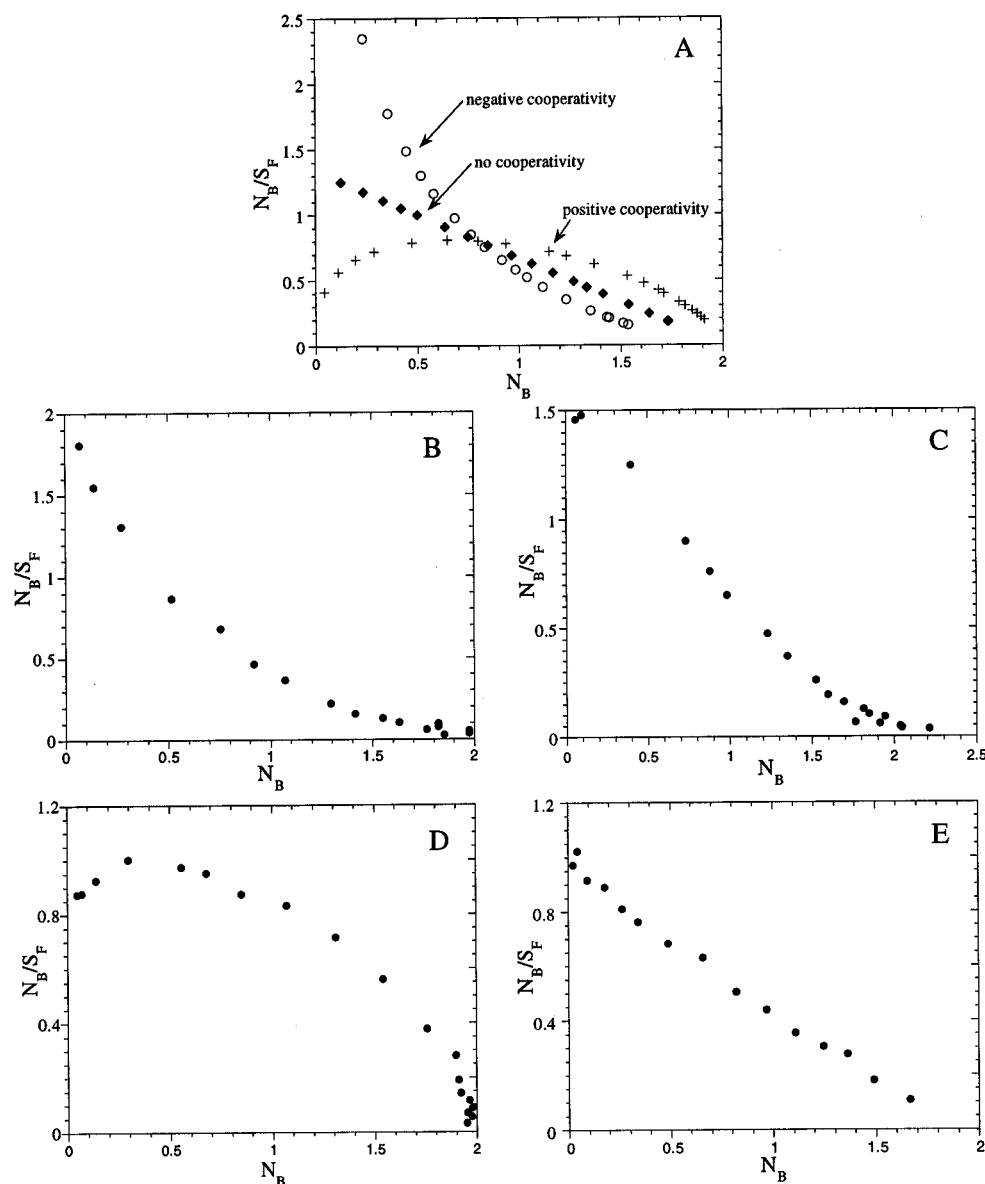


FIGURE 2: Scatchard plots for substrate binding. (A) Simulated data derived from the Hill equation (eq 2) and replotted with the Scatchard equation (eq 1). Data were simulated for a dimeric protein binding with full-sites occupancy at two sites with values of  $K_H = 0.67$  mM, and  $n_H = 0.7$  (○),  $n_H = 1.0$  (◆), and  $n_H = 1.5$  (+). Scatchard plots for experimental values (single experiments) measuring aspartate binding to (B) wild-type TarS, (C) S68C, (D) S68I, and (E) S68A. Counting errors on each point were no more than  $\pm 3\%$ .

Table 2: Best Fit Parameters Derived from the Sequential Model for the Experimentally Observed Binding Data of the *S.t.* Aspartate Receptor (Wild Type and Ser68 Substituted Mutants)

amino acid at position 68	best fit parameters <sup>a</sup>		
	$\varphi_1$	$\varphi_2$	$p_n$
serine (wt)	$1.4 \pm 0.2$	$0.1 \pm 0.03$	$1.1 \pm 0.03$
cysteine	$1.0 \pm 0.5$	$0.1 \pm 0.09$	$1.0 \pm 0.04$
valine	$1.9 \pm 0.5$	$0.8 \pm 0.4$	$0.9 \pm 0.1$
aspartate	$0.3 \pm 0.09$	$0.02 \pm 0.01$	$0.5 \pm 0.07$
alanine	$1.2 \pm 0.3$	$0.3 \pm 0.2$	$0.9 \pm 0.1$
threonine	$0.7 \pm 0.1$	$0.3 \pm 0.2$	$1.2 \pm 0.01$
leucine	$0.7 \pm 0.2$	$0.4 \pm 0.4$	$1.4 \pm 0.2$
asparagine	$0.2 \pm 0.04$	$0.06 \pm 0.04$	$0.9 \pm 0.3$
isoleucine	$0.7 \pm 0.4$	$1.0 \pm 0.3$	$0.9 \pm 0.09$

<sup>a</sup>  $\varphi_1$  is in units of  $\mu\text{M}^{-1}$  and  $\varphi_2$  is in units of  $\mu\text{M}^{-2}$ , and these variables are defined in eqs 3 and 5.

from these fits are listed in Table 2, and the refined data, calculated from eqs 5 and 6, are shown in Table 3. The constants  $K_1'$  and  $K_2'$ , which measure ligand affinity of the first and second binding sites, are the experimentally

observed binding constants that have been corrected for statistical factors and were determined from the values  $\varphi_1$  and  $\varphi_2$ , obtained from curve fitting to eq 7.

The results obtained from fitting the data to the Hill equation (eq 2) and the sequential model (eq 7) and from the Scatchard analysis were found to be in good agreement. Wild-type receptor and the S68C receptor exhibited Hill coefficients less than 1.0 ( $n_H = 0.7 \pm 0.1$  and  $n_H = 0.8 \pm 0.05$ , respectively), and for both samples,  $K_1' \approx 3K_2'$ . The S68V aspartate binding data exhibited less pronounced cooperativity ( $n_H = 0.9 \pm 0.1$ ), and  $K_1'$  and  $K_2'$  were equal within experimental error. The S68I and S68N receptors, where positive cooperativity was observed by Scatchard analysis, had  $n_H = 1.4 \pm 0.2$  and  $n_H = 1.3 \pm 0.2$ , respectively. For these receptors,  $K_2' \geq 5K_1'$ . For S68T and S68L, the data indicated modest positive cooperativity ( $n_H = 1.2 \pm 0.1$ ), and fit to  $K_2' \approx 2K_1'$  for S68T and  $K_2' \approx 3K_1'$  for S68L. The S68A receptor exhibited linear Scatchard plots,  $K_1' = K_2'$ ,  $n_H = 1.0 \pm 0.1$ , and  $N_{B \max} = 1.8$ , so this

Table 3: Comparison of Aspartate Binding Constants for the *S.t.* Aspartate Receptor (Wild Type and Mutants) Derived from Fits to the Sequential Model and the Hill Equation

amino acid at position 68	sequential model <sup>a</sup>		Hill equation <sup>b</sup>	
	$K_1'$	$K_2'$	$n_H$	$N_{Bmax}$
serine (wt)	$0.7 \pm 0.1^c$	$0.2 \pm 0.05^d$	$0.7 \pm 0.1$	$2.0 \pm 0.2$
cysteine	$0.5 \pm 0.2$	$0.2 \pm 0.08$	$0.8 \pm 0.02$	$2.1 \pm .08$
valine	$1.0 \pm 0.3$	$0.8 \pm 0.5$	$0.9 \pm .05$	$1.8 \pm 0.2$
aspartate	$0.1 \pm 0.03$	$0.1 \pm 0.04$	$1.0 \pm 0.1$	$1.0 \pm 0.1$
alanine	$0.6 \pm 0.1$	$0.6 \pm 0.3$	$1.0 \pm 0.03$	$1.8 \pm 0.1$
threonine	$0.4 \pm 0.03$	$0.9 \pm 0.1$	$1.2 \pm 0.09$	$2.4 \pm 0.02$
leucine	$0.3 \pm 0.1$	$1.1 \pm 1.4$	$1.2 \pm 0.1$	$2.6 \pm 0.2$
asparagine	$0.1 \pm 0.02$	$0.5 \pm 0.3$	$1.3 \pm 0.2$	$1.8 \pm 0.6$
isoleucine	$0.4 \pm 0.2$	$2.8 \pm 1.8$	$1.4 \pm 0.2$	$2.0 \pm 0.06$

<sup>a</sup> The binding constants  $K_1'$  and  $K_2'$  are expressed in units of  $\mu\text{M}^{-1}$  and were calculated from the parameters  $\varphi_1$  and  $\varphi_2$  (Table 2), obtained from fits to the sequential model (eq 7), as follows:  $K_1' = \varphi_1/2$  and  $K_2' = 2\varphi_2/\varphi_1$ . <sup>b</sup> Best fit binding parameters to the Hill equation were derived from eq 2. <sup>c</sup> The uncertainty in  $K_1'$  is  $\delta K_1' = \delta\varphi_1/2$ , and  $\delta\varphi_1$  is the uncertainty in  $\varphi_1$ . <sup>d</sup> The uncertainty in  $K_2'$  is  $\delta K_2' = K_2'[(\delta\varphi_1/\varphi_1)^2 + (\delta\varphi_2/\varphi_2)^2]^{1/2}$ , and  $\delta\varphi_2$  is the uncertainty in  $\varphi_2$ .

receptor showed no cooperativity. In the case of S68D, binding at only one site could be detected. The Scatchard plots converged to an abscissa value of  $N_{B \max} \approx 1$ , and the fits to the Hill equation yielded an occupancy of  $1.0 \pm 0.1$  aspartates bound per receptor dimer. A best fit to eq 7 was obtained with  $\varphi_1 = 0.3 \pm 0.09$ ,  $\varphi_2 = 0.02 \pm 0.01$ , and  $p_n = 0.5$ , also indicating that the binding data for S68D are best described by a single binding constant,  $K_1' = 0.1 \mu\text{M}^{-1}$ , and half-of-the-sites occupancy. Further attempts to detect binding at the second site using higher substrate concentrations (100–200  $\mu\text{M}$ ) were unsuccessful. The binding stoichiometries of all other Ser68 mutants yielded values close to 2.0, indicating full-sites occupancy. Binding affinities to the S68F, S68Q, and S68E receptors, however, were too weak to assess binding stoichiometry or cooperativity.

**Binding Affinity.** The aspartate binding constants of the wild-type aspartate receptor were compared with those of the mutants (Table 3). For many of the mutants, aspartate affinity for the first site did not change appreciably. For example, the  $K_1'$  value for wild-type receptor was  $0.7 \pm 0.1$ , about equal to the  $K_1'$  values of S68A ( $K_1' = 0.6 \pm 0.1$ ), S68I ( $0.4 \pm 0.2$ ), and S68V ( $1.0 \pm 0.3$ ). The strongest affinity occurred for the second aspartate molecule binding to S68I where positive cooperativity in this mutant enhanced binding of the second ligand 10-fold over wild type. Binding affinity was reduced about 7-fold in S68D and S68N. The decrease in  $K_1'$  in S68D cannot be attributed entirely to charge repulsions between the ligand  $\gamma$ -carboxylate and the Asp68 side chain since a similar binding constant was obtained in the Asn68 mutant. Negative cooperativity in S68D, perhaps mediated by electrostatic interactions, contributed to its overall lower aspartate affinity, in contrast to S68N where binding at the second site was enhanced and both sites were occupied readily. If a similar level of negative cooperativity occurred in S68D as with wild type, the estimated value of  $K_2'$  would be  $\leq 0.02 \mu\text{M}^{-1}$ , whereas  $K_2'$  was  $0.5 \pm 0.3 \mu\text{M}^{-1}$  for S68N.

No binding could be detected for the S68E, S68Q, and S68F mutants by the equilibrium binding method because the  $K_1'$ s were too small. However, an estimate of the binding constant was obtained by measuring the enhanced rate of methylation of the receptor by CheR as a function of

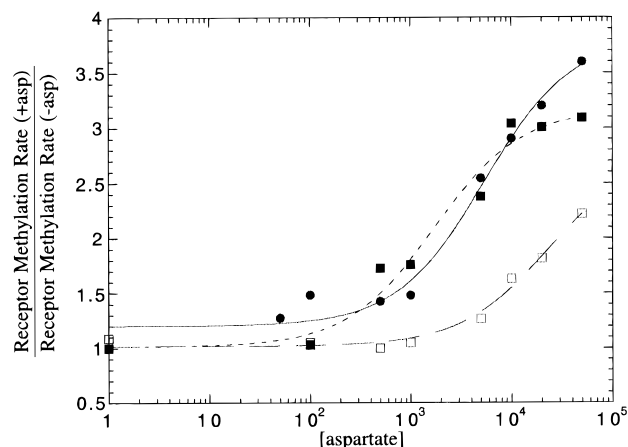


FIGURE 3: Plot of the relative rate of receptor methylation by CheR as a function of aspartate concentration. Rates for each mutant at a given aspartate concentration were referenced to the rate in the absence of aspartate (which was assigned a relative rate = 1.0). The lines are best fits to a Michaelis–Menten isotherm (eq 3). Error limits on each data point were approximately  $\pm 10\%$ . Mutants analyzed were S68F (circles; —), S68Q (filled squares; ---), and S68Q (open squares; - -).

aspartate concentration (Figure 3). For the wild-type receptor,  $K_{1/2}$ , the concentration of aspartate required for half-maximal stimulation of receptor methylation is close to the affinity measured by equilibrium binding (Mowbray & Koshland, 1990). The value of  $K_{1/2}$  obtained by this method was 5.4 mM for S68F, 1.7 mM for S68Q, and  $\geq 23$  mM for S68E, corresponding to a decrease in aspartate affinity of roughly 1600-fold, 500-fold, and 7000-fold, respectively.

The lack of binding in the S68F substitution is logical since the phenylalanine side chain should provide a substantial disruption of the intersubunit interface. Neighboring aromatic rings in protein interiors prefer to pack at 4.5–7 Å separations at dihedral angles approaching 90° (Burley & Petsko, 1985). Packing of the large Phe68 and Phe68' side chains (135 Å<sup>3</sup>) in this configuration, and even in more compact arrangements, can only be accommodated by large backbone movements of the two helices that form the interface and the two binding sites.

Modeling of the Glu68 mutation into the X-ray structure of the ligand binding domain indicated that electrostatic repulsion is in large part responsible for the weak aspartate binding of S68E. This substitution would place the  $\delta$ -carboxyl of Glu68 close to both the aspartate  $\gamma$ -carboxyl ( $d_{O-O} = 3.6$  Å) and  $\alpha$ -carboxyl ( $d_{O-O} = 2.6$  Å). It is also possible that Glu68 might form an ion pair with either Arg64 or Arg69', key binding site ligands to aspartate, and compete with aspartate for this energetically favorable interaction. The modeled distance between the Glu68 and Arg64 was 3.9 Å ( $d_{O\delta-N\epsilon}$ ). Rotation of the arginine side chain about the C $\gamma$ –C $\delta$  ( $\sim 120^\circ$ ) and C $\delta$ –N $\delta$  ( $\sim 30^\circ$ ) bonds in the water-filled binding pocket would place it in a conformation where it could form a strong salt bridge with Glu68 while also sterically blocking access of aspartate. Similarly, a hydrogen-bonding interaction between Gln68 and Arg64 or Arg69' may also explain why this electrostatically neutral substitution is effective in reducing aspartate affinity to a similar extent. Steric disruption of the binding site by the Glu68 or Gln68 side chains may be of secondary importance since the side chain volumes of Gln and Glu (109 and 114 Å<sup>3</sup>) are very close to that of Ile (124 Å<sup>3</sup>) (Creighton, 1993), and

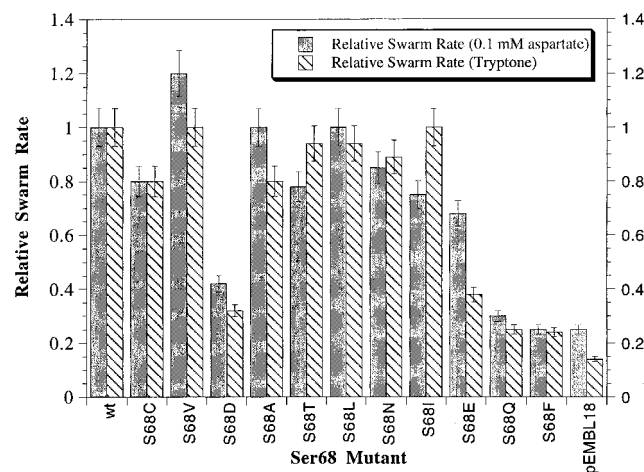


FIGURE 4: Relative swarm rates of wild-type and Ser68 aspartate receptor mutants, referenced to wild-type receptor (rate = 1.0). Relative swarm rates on minimal media supplemented with 0.1 mM aspartate (solid bars) and tryptone (hatched bars) are presented. The wild-type swarm rate was 0.5 mm/h on aspartate plates and 2.0 mm/h on tryptone plates.

the Ile68 mutant binds aspartate with high affinity. On the other hand, Gln and Glu are expected to extend more deeply into the binding pocket than Ile, and differences in the packing of these side chains within the binding pocket and at the subunit interface would alter the energy of unfavorable van der Waals contacts with the substrate.

**Receptor Aspartate Signaling Activity.** Swarm assays were conducted on 1% tryptone and on 0.1 mM aspartate to measure the ability of each mutant to mediate a chemotactic response (Figure 4). At this concentration of attractant, only receptors with substantially altered binding affinity will exhibit significant defects. Most of the substitutions produced functional receptors that mediated swarming behavior on tryptone and aspartate similar to that of the wild-type receptor. Despite changes in cooperativity, the mutants S68A, S68C, S68T, S68D, S68N, S68V, S68L, and S68I all bind aspartate at concentrations at least 10-fold lower than that included on the aspartate swarm plates. Of these, only S68D appeared to be defective and swarmed at rates 42% and 32% lower than that of wild type on tryptone and aspartate media, respectively. Three other mutants, S68F, S68E, and S68Q, exhibited markedly depressed swarm rates on both media, consistent with aspartate affinities in the millimolar range. The S68E mutant swarm rates on tryptone and aspartate were 38% and 68% of the wild-type levels, respectively, and the S68Q and S68F swarm rates were close to that of the negative control (pEMBL18 vector).

The mutations do not seem to damage the receptor conformation. Methylation of the aspartate receptor by the SAM-dependent methyl transferase, CheR, occurs at four glutamate residues in the cytoplasmic domain and is stimulated by aspartate binding. Proper folding of the receptor is required for efficient receptor methylation, and the degree of aspartate stimulation is a good indicator of receptor signaling activity. In the absence of aspartate, all of the receptor mutants are methylated by CheR at rates comparable to that of wild type, indicating that they have a native receptor structure. The level of stimulation of CheR activity by 1 mM aspartate correlated somewhat with the mode of binding cooperativity (Figure 5). Overall, stimulation of the methylation rate was somewhat higher for the receptors exhibiting

positive cooperativity than for the mutants binding with negative and no cooperativity. The acidic substitutions S68E, which exhibited low aspartate affinity, and S68D, which bound aspartate with half-of-the-sites occupancy, had significantly lower stimulation levels than that of wild type. Aspartate stimulation of methylation for the other low-affinity receptors, S68F and S68Q, along with S68E, was enhanced at higher aspartate concentrations, and stimulation of the CheR methylation rate by 3.6-fold (S68F), 3.0-fold (S68Q), and 2.0-fold (S68E) was observed at 50 mM aspartate.

## DISCUSSION

This mutagenesis study has further defined the functional role of Ser68 in the aspartate receptor of *S. typhimurium*. This residue is at a critical position in the binding site and is poised at the switch point between ligand binding and intersubunit conformational changes. Substitutions at this single site can alter the type of cooperativity and switch cooperativity from negative to positive. The results of the S68A mutation demonstrate the role of Ser68 in cooperativity most dramatically. Cooperativity was abolished with the simple removal of the serine  $\beta$ -hydroxyl group, a change that eliminated any Ser68–Ser68' hydrogen bond and left only a weak van der Waals interaction. Scatchard plots of aspartate binding to S68A were linear and corresponded to full-sites occupancy. Moreover, binding curves fit to a Hill coefficient,  $n_H = 1.0$ , and the intrinsic constants,  $K_1'$  and  $K_2'$ , were equal. Importantly, the signaling properties of this receptor were not appreciably altered, indicating that this receptor folded into a wild-type conformation. It was fully functional in chemotaxis swarm plate assays, and the rate of receptor methylation by CheR was stimulated by aspartate at levels equal to that of wild type. The results of this mutation further support the conclusion of Biemann and Koshland (1994) that negative cooperativity in this receptor is due to allosteric interactions rather than an artifact resulting from a mixed population of receptors and other proteins with different conformations and binding affinities. If the latter explanation were true, it is unlikely that we would have observed an effect on cooperativity from the S68A mutation since this single residue change would not be expected to affect the heterogeneity of the receptor and protein population. Positive cooperativity, exhibited by other mutants, would also not be observable if a mixed population of binding sites persisted.

The results indicate that small changes in amino acid residues can dramatically change cooperativity without changing the absolute values of  $K_1'$  and  $K_2'$  greatly. Positive or negative cooperativity is tuned with great sensitivity by the amino acid at position 68. Comparing the branched-chain amino acids valine and isoleucine which differ by a single methylene carbon, the former displayed negative cooperativity whereas the latter exhibited strong positive cooperativity. Similarly, changing serine to threonine, a difference of a methyl group, also switched binding behavior from negative to positive cooperativity. Changes in charge can also have dramatic effects on cooperativity. Mutation to a negatively charged aspartate conserved negative cooperativity but resulted in the extreme form of negative cooperativity, half-of-the-sites binding, and we estimate that  $K_1' > 7K_2'$  for S68D. However, the analogous neutral mutant, S68N, binds aspartate with pronounced positive cooperativity and  $K_2' = 5K_1'$ . These results prove that the identity of the

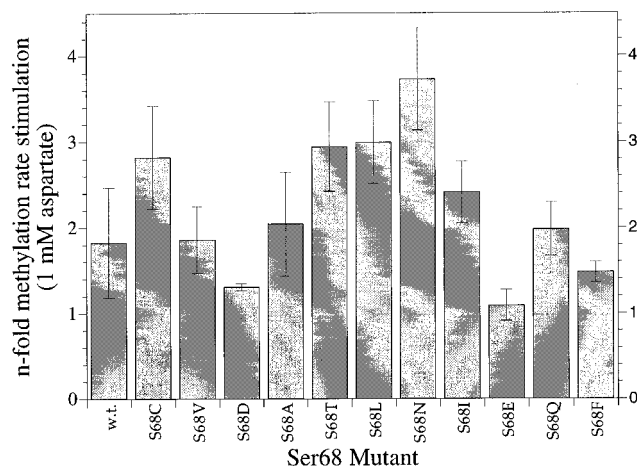


FIGURE 5: Stimulation of receptor methylation by CheR, induced by 1 mM aspartate, for wild-type aspartate receptor and Ser68 mutants. The receptors are listed left to right in order of increasing Hill coefficient, except for S68E, S68Q, and S68F.

residue at position 68 can determine the mode and extent of cooperativity. Cooperative behavior is extremely sensitive to subtle changes in the packing of this residue that is located at the interface of the two subunits. The effects of these diverse mutations suggest that individual substitutions could mediate allostery by different mechanisms.

Serine 68 is one of three residues, along with the two arginines donated by the opposite subunit, Arg69' and Arg73', that are located both within the primary shell of residues in the binding site and at the subunit interface. In contrast to the arginine residues which make strong, proximal electrostatic bonds with aspartate, the hydroxyl group of Ser68 is positioned too far from the ligand aspartate to form direct contacts. Instead, it interacts with the aspartate via hydrogen bonds to two water molecules which coordinate the  $\alpha$ -carboxyl and  $\gamma$ -carboxyl of aspartate. Serine 68 is also unique among the binding site residues in that it is poised at the interface of the two subunits such that it packs close to Ser68' at a  $C_{\beta}$ – $C_{\beta}$ ' bond distance of 3.53 Å. The strength of the hydrogen-bonding interactions of Ser68 with aspartate

ligated water molecules in the binding site is likely to be important for determining the orientation of this side chain toward either the binding pocket or the subunit interface. Molecular modeling studies indicate that there is ample space in the structure to allow rotation of the  $C_{\alpha}$ – $C_{\beta}$  bonds so as to bring the side chains into a conformation that would form an intersubunit hydrogen bond. Such interactions could be the basis for the cooperativity observed upon aspartate binding in the wild-type receptor.

A remarkable feature of the structure of the aspartate-bound periplasmic domain is that only one site was fully occupied by aspartate, even though apparently saturating substrate concentrations were used in crystallizing the complex (Milburn et al., 1991; Yeh et al., 1993). A third, more refined structure of the wild-type periplasmic domain, termed here the doubly occupied form, was recently determined from a crystal grown at higher aspartate concentration and showed partial occupancy by aspartate at the second, "weak" site (Yeh et al., 1996). The one aspartate-bound structure may be considered to be intermediate between apo and fully bound receptor, and changes in these structures are important for understanding the mechanism of negative cooperativity.

Ligand-induced differences in binding affinity could be caused by direct changes to side chain orientations at the second site or to changes that create a more stable interface between the subunits in the half-occupied as compared to the fully bound form. We observe evidence of both mechanisms. A superposition of the residues composing the two binding sites and a portion of the protein interface (amino acids 64–73, 64'–73', 148–156, 148'–156'; 152 atoms) in the three forms of the aspartate receptor periplasmic domain indicated that changes in the position of the protein backbone were small (Figure 6). The root-mean-square deviation was 0.32 Å between the apo and half-of-the-sites forms, 0.31 Å between the apo and doubly occupied forms, and 0.15 Å between the half-of-the-sites and doubly occupied forms. However, there were substantial movements of the protein side chains in the binding pockets, the largest of which (0.3–0.6 Å) occurred when the first site was occupied by aspartate.

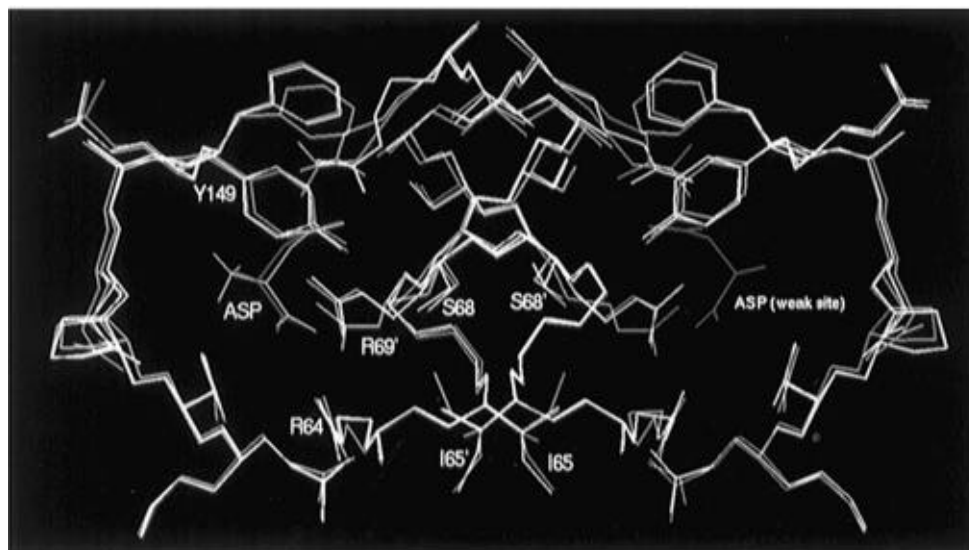


FIGURE 6: Least squares superposition of the binding sites of the apo (magenta), half-of-the-sites occupied (green), and doubly occupied (yellow) aspartate receptor structures. Backbone atoms of residues 64–73, 64'–73', 148–156, and 148'–156' were compared. Aspartate is shown in orange in the half-of-the-sites structure and in red in the doubly occupied form. In the doubly occupied form, partial occupancy of the "weak" site is observed.



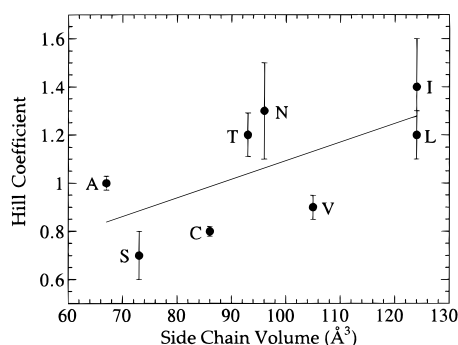


FIGURE 7: Plot of the Hill coefficient as a function of side chain volume ( $\text{\AA}^3$ ).  $n_H$  for each mutant was calculated from eq 2 (and listed in Table 3). The mutant S68D was excluded from the plot since it exhibits half-of-the-sites binding.

These subtle perturbations to the position and conformation of residues interacting with aspartate could account for the 3-fold difference between  $K_1'$  and  $K_2'$ , about 0.7 kcal/mol in binding energy, observed in the wild-type receptor.

Aspartate binding also resulted in changes to side chain conformations at the protein interface, including the side chain of Ser68. The distance between the serine  $\beta$ -methylene carbons changed from 3.53  $\text{\AA}$  in the apo form to 3.34  $\text{\AA}$  after binding of one aspartate and was extended to 3.83  $\text{\AA}$  in the doubly occupied form. Upon binding of the second aspartate, a hydrogen bond between the Ser68'  $\beta$ -hydroxyl and the backbone carbonyl of Ile65' was broken, and a hydrogen bond with an aspartate-bound water was formed. The side chains of Ile65 and Ile65' also rotated ( $C_\beta$ – $C_\gamma$  bond) into a more compact arrangement upon binding of the first aspartate, suggesting that this residue may also be important for cooperativity.

Overall, the packing at the interface becomes more compact upon binding of aspartate, as measured by a decrease in solvent accessibility to the half-of-the-sites dimer of 85  $\text{\AA}^2$ , as compared to the apo dimer (Yeh et al., 1996). If interactions between Ser68 and Ser68' are important for stabilizing this interface, a substitution that would reduce them would be expected to alter cooperativity. The S68A mutant introduces a pair of residues at the subunit interface that are 3.5  $\text{\AA}$  apart. Van der Waals interactions will be weak, steric disruption of the subunit interface is expected to be negligible, and indeed, no cooperativity is observed.

If closer packing of the interface contributes to negative cooperativity, mutations that would disrupt close packing should result in positive cooperativity. The space occupied by Ser68 is tightly packed, and substitutions at this position with branched chain amino acids cannot be accommodated without some movement of the protein backbone and nearby side chains. Large residues would cause local bulging around position 68 and maintain a greater separation between the two binding sites. In correlating the size of the side chain at residue 68 with the Hill coefficient, we observe an overall increase in positive cooperativity with increase in side chain volume (Figure 7). The residues isoleucine and leucine have side chain volumes 51  $\text{\AA}^3$  larger than serine and would tend to pack against each other so as to maximize van der Waals interactions. Such an arrangement is in fact observed for Ile65 and Ile65', which are located one helical turn away from residue 68. Ile68 or Leu68 could pack against the Ile65 pairs to form an expanded, stable hydrophobic core, and rearrangements of these residues, energetically driven by

aspartate binding, could account for the observed positive cooperativity. Fitting the Ile68 or Leu68 residues into the structure requires movement of the two  $\alpha$ -helices containing residues 68 and 68', and the degree of disruption of the subunit interface would increase with increased van der Waals interaction between these residues. Gross changes at the interface, however, would be expected to affect positioning in the binding site of Arg69' and Arg73', residues essential for aspartate recognition, resulting in far more substantial decreases in affinity than are observed. Size and steric factors may be relevant for explaining the effects of some substitutions, but no immediate correlation with cooperativity is obtained ( $R = 0.67$ ). No simple linear relationships emerge when direct comparisons are made (Thr vs Val; Asp vs Asn), suggesting the importance of other parameters, such as electrostatic and hydrogen-bonding interactions.

The current work demonstrates that mutations at a single site can modulate cooperativity in a protein while also exerting only moderate effects on substrate binding affinity. Previous experiments in other systems such as hemoglobin [see Perutz (1990) for a review] have demonstrated that positive cooperativity can be abolished or conferred to an enzyme or protein by a single site mutation. Such studies have also involved mutations at subunit interfaces. For example, when Gly418 of the dimeric *E. coli* enzyme glutathione reductase, located in a closely packed region of the interface, is replaced with a bulky tryptophan residue, the enzyme becomes highly cooperative (Scrutton et al., 1992). The Hill coefficient is increased from 1.00 to 1.76 with only small effects on  $K_m$  and  $k_{cat}$ . Some of the effects can be more complex. In the multisubunit enzyme aspartate transcarbamoylase of *E. coli*, numerous mutations of residues involved in interdomain contacts result in loss or gain of homotropic and heterotropic cooperativity but also frequently reduce catalytic efficiency significantly (Dembowski et al., 1990; Eisenstein et al., 1990; Stevens et al., 1991; Newton et al., 1992). Other instances of reduction in positive cooperativity have been reported in systems such as hemoglobin (Valdes & Ackers, 1977; Perutz, 1990; Ishimori et al., 1992), cAMP-dependent protein kinase I (Bubis et al., 1988), lac repressor (Chang et al., 1993), and GroES (Kovalenko et al., 1994).

Most of our mutations had only small effects on aspartate affinity. Binding affinity in the first site was only marginally affected by removal of the Ser68  $\beta$ -hydroxyl, as in the S68A mutant. It is possible that an additional water molecule might have substituted for the missing serine hydroxyl, obscuring the energetic contribution of a Ser68-mediated hydrogen bond. In the enzyme thymidylate synthase, an arginine residue thought to be important for coordinating the phosphate moiety of UDP was replaced by alanine with little effect on substrate binding because the binding capacity of the guanido group was fulfilled by three water molecules occupying positions similar to the arginine nitrogens (Santi et al., 1990; J. Finer-Moore, personal communication).

Other aliphatic substitutions in the aspartate receptor, S68V, S68I, and S68L, also had small differences in affinity from that of wild type, and some actually had higher binding affinity. Small perturbations to the structure around the active site, including the bound water molecules, could readily explain the observed changes in binding energy. On the other hand, very bulky substitutions at position 68, such

as Phe and Gln, and acidic residues, Asp and Glu, substantially reduce binding. Modeling of Phe into the crystal structure indicated that this residue would disrupt the protein interface and hence affect proper alignment of residues in the binding pocket. Gln was found to sterically block access of aspartate to the binding site. Electrostatic repulsions can explain the decrease in ligand affinity observed for S68D and S68E.

Negative cooperativity has been conserved in the aspartate receptor at the expense of higher affinity. The construction of mutants with somewhat enhanced aspartate binding affinity indicates that the aspartate receptor has not been optimized for aspartate binding. The Ser68 substitutions Val, Thr, Leu, and Ile all yield receptors with somewhat higher overall aspartate affinity. Binding at the second site in the S68I receptor, for example, is over 10-fold better than that of wild type, but cooperativity has been changed significantly. Conservation of negative cooperativity may optimize the chemotactic response. By binding and reacting to aspartate concentrations at two different apparent affinities, negative cooperativity expands, in principle, the range over which the aspartate receptor can be used to sense changes in an aspartate gradient and desensitizes the receptor to small concentration fluctuations. Negative cooperativity would also result in activation of more receptor dimers at low concentrations of attractant, perhaps amplifying an aspartate signal. For the *E. coli* aspartate receptor, which also mediates chemotaxis toward maltose in conjunction with the maltose binding protein, half-of-the-sites reactivity may enable this receptor to generate independent signals toward these substrates (Mowbray & Koshland, 1987; Stoddard & Koshland, 1992; Biemann & Koshland, 1994).

These mutagenesis experiments reveal the sensitive tuning required in designing the protein interface and binding pocket so as to conserve both high affinity and cooperativity. The ability to change cooperativity from negative to positive with a single amino acid change has consequences for the evolution of protein regulation. For organisms to adapt to different conditions, ligand affinity of a given protein must frequently be altered. For example, the tadpole expresses a different hemoglobin than that of the frog. The tadpole and frog hemoglobins possess a pair of key amino acid substitutions that result in substantial changes to their allosteric properties (Perutz & Brunori, 1982; Brunori et al., 1985). Frogs exist in an environment with much higher oxygen concentration than the tadpole, and their respective hemoglobins have different oxygen binding properties that compensate for changes in environment and physiology (Kay et al., 1980; Williams et al., 1980; Banville et al., 1983; Andres et al., 1984). Creating a new heme binding pocket specific for oxygen by mutations within the binding pocket could result in drastic changes that might not produce the fine tuning required for frog development and could have more widespread, deleterious consequences. Mutations remote from the binding pocket which affect allostery, on the other hand, can change affinity and oxygen binding behavior without redesigning the active site (Koshland, 1976). This work with mutations at a single site in the aspartate receptor further illustrates how readily mutations that alter the cooperativity pattern can be acquired in ways that can provide great evolutionary advantage in metabolism.

## REFERENCES

- Andres, A. C., Hosbach, H. A., & Weber, R. (1984) *Biochim. Biophys. Acta* 781, 294–301.
- Banville, D., Kay, R. M., Harris, R., & Williams, J. G. (1983) *J. Biol. Chem.* 258, 7924–7927.
- Barford, D., & Johnson, L. N. (1990) *Nature (London)* 340, 609–616.
- Biemann, H.-P., & Koshland, D. E., Jr. (1994) *Biochemistry* 33, 629–634.
- Browner, M. F., Hackos, D., & Fletterick, R. (1994) *Nat. Struct. Biol.* 1, 327–333.
- Brunori, M., Condo, S. G., Bellelli, A., Giardina, B., & Micheli, G. (1985) *J. Mol. Biol.* 181, 327–329.
- Bubis, J., Saraswat, L. D., & Taylor, S. S. (1988) *Biochemistry* 27, 1570–1576.
- Burley, S. K., & Petsko, G. A. (1985) *Science* 269, 23–28.
- Chang, W.-L., Olson, J. S., & Matthews, K. S. (1993) *J. Biol. Chem.* 268, 17613–17622.
- Clarke, S., & Koshland, D. E., Jr. (1979) *J. Biol. Chem.* 254, 9695–9702.
- Creighton, T. E. (1993) *Proteins: Structures and Molecular Properties*, 2nd ed., W. M. Freeman and Co., New York, NY.
- Dahlquist, F. W. (1978) *Methods Enzymol.* 48, 270–299.
- Dembowski, N. J., Newton, C. J., & Kantrowitz, E. R. (1990) *Biochemistry* 29, 3716–3723.
- Dente, L., Cesareni, G., & Cortese, R. (1983) *Nucleic Acids Res.* 11, 1145–1655.
- Eisenstein, E., Markby, D. W., & Schachman, H. K., (1990) *Biochemistry* 29, 3724–3731.
- Falke, J. J., & Koshland, D. E., Jr. (1987) *Science* 237, 1596–1600.
- Foster, D. L., Mowbray, S. L., Jap, B. K., & Koshland, D. E., Jr. (1985) *J. Biol. Chem.* 260, 11706–11710.
- Gardina, P., Conway, C., Kossman, M., & Manson, M. (1992) *J. Bacteriol.* 174, 1528–1536.
- Gouaux, J. E., Stevens, R. C., & Lipscomb, W. N. (1990) *Biochemistry* 29, 7702–7715.
- Hill, A. V. (1910) *J. Physiol. (London)* 90, iv–vii.
- Ho, C. (1992) *Adv. Protein Chem.* 43, 153–312.
- Innis, M. A., Myambo, K. B., Gelfand, D. H., & Brow, M. A. D. (1988) *Proc. Natl. Acad. Sci. U.S.A.* 85, 9436–9440.
- Ishimori, K., Imai, K., Miyazaki, G., Kitagawa, T., Wada, Y., Morimoto, H., & Morishima, I. (1992) *Biochemistry* 31, 3256–3264.
- Kantrowitz, E. R., & Lipscomb, W. N. (1990) *Trends Biochem. Sci.* 15, 53–59.
- Kay, R. M., Harris, R., Patient, R. K., & Williams, J. G. (1980) *Nucleic Acids Res.* 8, 2691–2707.
- Ke, H., Lipscomb, W. N., Cho, Y., & Honzatko, R. B. (1988) *J. Mol. Biol.* 204, 725–748.
- Klotz, I. M. (1982) *Science* 217, 1247–1249.
- Koshland, D. E., Jr. (1975) in *The Enzymes* (Boyer, H., Ed.) 3rd ed., Vol. 1, pp 341–396, Academic Press, Inc., New York, NY.
- Koshland, D. E., Jr. (1976) *Fed. Proc.* 35, 2104–2111.
- Koshland, D. E., Jr., Nemethy, G., & Filmer, D. (1966) *Biochemistry* 5, 365–385.
- Kossman, M., Wolff, C., & Manson, M. D. (1988) *J. Bacteriol.* 170, 4516–4521.
- Kossman, R. P., Gouaux, J. E., & Lipscomb, W. N. (1993) *Proteins* 15, 147–176.
- Kovalenko, O., Yifrach, O., & Horovitz, A. (1994) *Biochemistry* 33, 14974–14978.
- Krause, K. L., Volz, K. W., & Lipscomb, W. N. (1987) *J. Mol. Biol.* 193, 527–553.
- Kunkel, T. A. (1985) *Proc. Natl. Acad. Sci. U.S.A.* 82, 488–492.
- Laemmli, U. K. (1970) *Nature (London)* 227, 680–685.
- Levitzi, A., & Koshland, D. E., Jr. (1969) *Proc. Natl. Acad. Sci. U.S.A.* 62, 1121–1128.
- Levitzi, A., Stallcup, W. B., & Koshland, D. E., Jr. (1971) *Biochemistry* 10, 3371–3378.
- Liu, J., & Parkinson, S. (1989) *Proc. Natl. Acad. Sci. U.S.A.* 86, 8703–8707.
- Milburn, M. V., Privé, G. G., Milligan, D. L., Scott, W. G., Yeh, J., Jancarik, J., Koshland, D. E., Jr., & Kim, S.-H. (1991) *Science* 254, 1342–1347.

- Miura, S., & Ho, C. (1982) *Biochemistry* 21, 6280–6287.
- Miura, S., & Ho, C. (1984) *Biochemistry* 23, 2492–2499.
- Miura, S., Ikeda-Saito, M., Yonetani, T., & Ho, C. (1987) *Biochemistry* 26, 2149–2155.
- Monod, J. L., Wyman, J. P., & Changeux, J. P. (1965) *J. Mol. Biol.* 12, 88–118.
- Mowbray, S. L., & Koshland, D. E., Jr. (1987) *Cell* 50, 171–180.
- Mowbray, S. L., & Koshland, D. E., Jr. (1990) *J. Biol. Chem.* 265, 15638–15643.
- Newton, C. J., Stevens, R. C., & Kantrowitz, E. R. (1992) *Biochemistry* 31, 3026–3032.
- Perutz, M. F. (1970) *Nature (London)* 228, 726–739.
- Perutz, M. F. (1990) *Mechanisms of Cooperativity and Allosteric Regulation in Proteins*, Cambridge University Press, Cambridge, England.
- Perutz, M. F., & Brunori, M. (1982) *Nature (London)* 299, 421–426.
- Perutz, M. F., Fermi, G., Luisi, B., Shaanan, B., & Liddington, R. (1987) *Acc. Chem. Res.* 20, 309–321.
- Santi, D. V., Pinter, K., Kealey, J., & Davisson, V. J. (1990) *J. Biol. Chem.* 265, 6770–6775.
- Scatchard, G. (1949) *Ann. N.Y. Acad. Sci.* 51, 660–672.
- Scrutton, N. S., Deonarain, M. P., Berry, A., & Perham, R. N. (1992) *Science* 258, 1140–1143.
- Shapiro, M. J., & Koshland, D. E., Jr. (1994) *J. Biol. Chem.* 269, 11054–11059.
- Simms, S. A., Stock, A. M., & Stock, J. B. (1987) *J. Biol. Chem.* 262, 8537–8543.
- Stevens, R. C., & Lipscomb, W. N. (1992) *Proc. Natl. Acad. Sci. U.S.A.* 89, 5281–5285.
- Stevens, R. C., Gouaux, J. E., & Lipscomb, W. N. (1990) *Biochemistry* 29, 7691–7701.
- Stevens, R. C., Chook, Y. M., Cho, C. Y., Lipscomb, W. N., & Kantrowitz, E. R. (1991) *Protein Eng.* 4, 391–408.
- Stoddard, B. L., & Koshland, D. E., Jr. (1992) *Nature* 358, 774–776.
- Valdes, R., & Ackers, G. M. (1977) *J. Biol. Chem.* 252, 88–93.
- Weis, R. M., & Koshland, D. E. (1990) *J. Bacteriol.* 172, 1099–1105.
- Williams, J. G., Kay, R. M., & Patient, R. K. (1980) *Nucleic Acids Res.* 8, 4247–4258.
- Wolfe, A. J., Conley, M. P., & Berg, H. C. (1988) *Proc. Natl. Acad. Sci. U.S.A.* 85, 6711–6715.
- Wolff, C., & Parkinson, J. S. (1988) *J. Bacteriol.* 170, 4509–4515.
- Yeh, J. I., Biemann, H.-P., Pandit, J., Koshland, D. E., Jr., & Kim, S.-H. (1993) *J. Biol. Chem.* 268, 9787–9792.
- Yeh, J. I., Biemann, H.-P., Prive, G., Pandit, J., Koshland, D. E. Jr., & Kim, S.-H. (1996) *J. Mol. Biol.* 262, 186–201.
- Zhang, Y., Liange, J.-Y., Huang, S., & Lipscomb, W. N. (1994) *J. Mol. Biol.* 244, 609–624.

BI961481V